

See discussions, stats, and author profiles for this publication at: <https://www.researchgate.net/publication/229942398>

Simulation of Oriented Collision Dynamics of Simple Chiral Molecules

ARTICLE in INTERNATIONAL JOURNAL OF QUANTUM CHEMISTRY · JUNE 2011

Impact Factor: 1.43 · DOI: 10.1002/qua.22816

CITATIONS

18

READS

15

5 AUTHORS, INCLUDING:



Federico Palazzetti

Università degli Studi di Perugia

35 PUBLICATIONS 339 CITATIONS

SEE PROFILE



Guilherme Maciel

82 PUBLICATIONS 706 CITATIONS

SEE PROFILE



Vincenzo Aquilanti

Università degli Studi di Perugia

315 PUBLICATIONS 6,403 CITATIONS

SEE PROFILE



Mikhail Borisovich Sevryuk

Russian Academy of Sciences

93 PUBLICATIONS 1,160 CITATIONS

SEE PROFILE

Simulation of Oriented Collision Dynamics of Simple Chiral Molecules

A. LOMBARDI,¹ F. PALAZZETTI,¹ G. S. MACIEL,¹ V. AQUILANTI,¹
M. B. SEVRYUK²

¹*Dipartimento di Chimica, Università di Perugia, Via Elce di Sotto 8, 06123 Perugia, Italy*

²*Institute of Energy Problems of Chemical Physics, The Russia Academy of Sciences,
Leninskiĭ prospect 38, Building 2, Moscow 119334, Russia*

Received 21 February 2010; accepted 14 April 2010

Published online in Wiley InterScience (www.interscience.wiley.com).

DOI 10.1002/qua.22816

ABSTRACT: With the aim of illustrating computationally the mechanism of chiral discrimination induced by molecular collisions, we present results of extensive classical dynamics simulations of oriented collisions of rare gas atoms with prototypical chiral molecules, such as hydrogen peroxide and hydrogen persulfide. Models for the intermolecular and intramolecular interactions are based on previous quantum chemical calculations. The phenomenon of right-left asymmetry in scattering directions is documented both by exemplary single trajectories and by angular distributions obtained by statistical averagings. © 2010 Wiley Periodicals, Inc. *Int J Quantum Chem* 00: 000–000, 2010

Key words: molecular chirality; oriented collisions

1. Introduction

The phenomenon of chirality (handedness) occurs for molecular systems that can exist in two forms differing by being mirror images of each other (enantiomers). It has numerous and interesting implications in chemistry and biochemistry, especially concerning the role of specific enantiomers in reactions proceeding enantio-selectively, when

chiral reactants or catalysts are involved, or in the presence of external chiral fields. Amazingly, terrestrial life involves only the L enantiomers of amino acids and the D enantiomers of sugars, a fact known as the homochirality of life. The puzzling problems related to the origin of homochirality in nature have encouraged long-standing efforts to clarify its origin [1] and a long-lasting search for mechanisms responsible for the generation of enantiomeric excess.

Reactions can proceed enantio-selectively if chiral reactants or catalysts are involved, or if some external chiral perturbation is present, so the explanation for the homochirality is likely to be in an enantio-selective process. The attention so far has been mainly focused on the influence of some external

Correspondence to: A. Lombardi; e-mail: abulafia@dyn.unipg.it

Contract grant sponsor: MIUR (PRIN funding program).

Contract grant sponsor: ASI.

Contract grant sponsor: CINECA.

chiral fields. These are, for example, circularly polarized light but also magnetic optical activity (unpolarized light in a parallel magnetic field) of photochemical reaction products [2], occurring in principle in all media, has been considered as capable to induce enantio-selectivity in chemical reactions.

A reliable hypothesis for these mechanisms, but still not sufficiently investigated, attributes chirality discrimination to molecular collisions, and has been discussed in Ref. [3, 4], where it has been examined also the possibility that collisions take place in environments characterized by rotary or whirling motions [5–7]. This hypothesis can be verified combining experimental and theoretical efforts exploiting, as a starting point, previous results on collisional alignment in gaseous streams, such as those obtained in our laboratory in Perugia. The experiments involving molecular beams techniques can be assisted by model system simulations, permitting measurements or calculations of kinetic parameters (cross sections and rate constants) to be used in models to verify to which extent molecular collision mechanisms can induce chirality discrimination and play a role in chirality manifestations [8].

The appropriate experimental techniques for the study of collisional mechanisms are based on controlling the spatial orientation of molecules, particularly on intense continuous beams of aligned molecules (see Ref. [9]). These techniques are promising to evolve and extend to explicitly deal with the study of chemical stereodynamics. In fact, the recent articles [10, 11] account for advances in the production of intense and continuous beams of aligned molecules, demonstrating that in the prototypical case of a seeded supersonic expansion of a beam of the disc-shaped benzene molecules, besides acceleration and cooling, orientation of the molecular plane also occurs because of the anisotropy of the intermolecular forces, which govern collisions [11, 12]. Previous studies on the collisional alignment of the rotational angular momentum of diatomic molecules regarded O_2 , for which the effect was probed by magnetic analysis [13, 14], and N_2 , for which the probe was molecular beam scattering [15]. Extensions to other hydrocarbons, particularly ethylene and acetylene, have been also demonstrated [12, 16].

Besides collisional alignment techniques, we mention those where an external field induces a “forced” alignment. These are the focusing in electric fields through the Stark effect, which can be either first- or second-order for linear molecules or only first-order for symmetric top molecules (the

latter stronger than the former), the use of polarized absorption (limited to optically favorable transitions in the molecular manifold), the brute force techniques, which use strong electrical or magnetic fields and are applicable only to rotationally relaxed molecules with permanent electric or magnetic dipole moments, and the alignment in intense nonresonant laser fields. These techniques are of interest to mimic the situation of naturally occurring fields, although this is controversial in protobiological models, being improbable the circumstance for the sophisticated experimental sources in the Universe. However, expectations are frustrated because of the lack of laboratory demonstrations (see comments and references in the recent article [17]). The same article and other key references (see Refs. [18–21] and references therein) can also be consulted for the intensely investigated mechanism for the origin of homochirality based on parity violation by the weak forces.

From a theoretical point of view, the reliability of a collisional mechanism for enantio-selectivity can be assessed by simulation of collisions involving chiral molecules. In previous work, we have extensively investigated peroxide and persulfide molecules stimulated by the interesting problem of large amplitude vibrations involving, in this case, the chirality change transitions associated with the torsional motions around the O–O [22] and S–S [23] bonds. A systematic series of quantum chemical studies has been undertaken on systems that play roles in biological and combustion chemistry, and in particular in the photochemistry of the minor components of the atmosphere [24], specifically hydrogen peroxide [25]. Further studies regarded several systems obtained by substitutions of the hydrogens in H_2O_2 by alkyl groups [26] and halogens [27] (for the analogous systems, H_2S_2 and disulfides, see Ref. [23]). Quantum chemistry has been proved to have reached the stage of accurately calculating, for these series of molecules, many characteristic features (dipole moment, equilibrium geometries, heights of barriers for the chirality changing mode), which are crucial for the intramolecular dynamics. Quantum dynamics calculations have also been performed to compute torsional levels and the temperature dependence of their distributions [22, 23]. For the H_2O_2 system, the intermolecular interactions with various molecules and ions (see Refs. [28–30]) and with itself (see Ref. [31] and references therein) have been investigated.

Recently, we also proposed potential energy surfaces for the H_2O_2 and H_2S_2 systems interacting

TABLE I
Equilibrium geometries and barriers for H₂O₂ and H₂S₂ at the MP2/aug-cc-pVTZ^a level.

Configuration	R_{HX} (Å)	R_{XX} (Å)	\angle_{HXX} (deg)	\angle_{HXXH} (deg)	<i>Cis</i> barrier (kcal mol ⁻¹)	<i>Trans</i> barrier (kcal mol ⁻¹)
H ₂ O ₂	0.9668 ^a (0.950 ± 0.005) ^b	1.4537 ^a (1.475 ± 0.004) ^b	99.6128 ^a (94.8 ± 2) ^b	112.5422 ^a (119.8 ± 3) ^b	7.3623 ^a (7.033 ± 0.071) ^d	1.1036 ^a (1.104 ± 0.011) ^d
H ₂ S ₂	1.3360 ^f (1.3410) ^c	2.0590 ^f (2.059) ^c	97.7 ^f (97.4) ^c	91.1 ^f (90.8) ^c	5.7268 ^f (5.6896) ^e	8.2142 ^f (8.055) ^e

^a Theoretical data from Ref. [25].

^b Experimental data from Ref. [36].

^c Experimental data from Ref. [37].

^d Experimental data from Ref. [38].

^e Experimental data from Ref. [39].

^f Theoretical data from Ref. [33].

with the complete series of noble gases along with a corresponding hyperspherical expansion fitting the *ab initio* data [32, 33]. This information is used in this article, where we propose the study of prototypical oriented collisions between rare gas atoms and the H₂O₂ and H₂S₂ molecules, to document manifestations of chirality in collisions.

The article is organized as follows. Section 2 presents the atom–semirigid-rotor model for the Rg (rare gas) + H₂O₂ and the Rg + H₂S₂ systems, as obtained from the potential energy surfaces proposed in Refs. [32, 33], along with their corresponding hyperspherical representations. Section 3 discusses how oriented collisions can be simulated and presents some numerical calculation details. Section 4 is devoted to the results and their discussion, while concluding remarks are in Section 5.

2. Models for Collisions of Simple Chiral Molecules with Rare Gases

2.1. INTRAMOLECULAR AND INTERMOLECULAR COORDINATES

In the Perugia laboratory, previous experimental investigations have been devoted to the interactions of H₂O [34] and H₂S [35] with rare gases, and corresponding theoretical studies have yielded complementary information on the interactions (specifically the anisotropies) with respect to molecular beam scattering experiments that measure essentially the isotropic forces [34]. Similar experimental information is not yet available for extension to H₂O₂ and H₂S₂, which are among the simplest molecules for which chirality enters into play. In view of this, quantum chemical studies of the Rg + H₂X₂ (X = O, S)

systems have been carried out to obtain the corresponding intermolecular potential energy surfaces [32, 33]. Table I reports the barrier heights and equilibrium geometries for the two molecules calculated in Refs. [32] and [33] and compared with available experimental information [36–39].

The considered systems involve five atoms and a correspondingly high number of degrees of freedom, so the introduction of suitable approximations is highly desirable. In this case, in view of the use of the potential energy surface in collision simulations, all of the intramolecular modes of the hydrogen peroxide and persulfide were considered to be frozen, except for the torsion motion around the O–O and S–S bonds. This assumption is justified by the fact that to stretching and bending vibrations are associated much higher frequencies than to torsion, which is a floppy-mode, and can be considered approximately separable. A periodic double well potential energy profile along the torsion coordinate connects the two chiral forms of the molecules, which are separated by two barriers corresponding to the molecular *cis* configuration (see Table I). The torsional energy is a function of the molecular dihedral angle coordinate designated as γ and ranging from 0 to 2π . The double well profile modifies because of the interaction of the molecular system with the atom, specifically as a function of the distance between the atom and the molecular center of mass and, in an averaged way, of the orientation of the molecule. Accordingly, the complete potential energy function for the interaction of each of the two molecules with rare gas atoms can be represented as a sum of two terms, one accounting for the intramolecular (internal) torsional energy and another one for the intermolecular (external) interaction energy, which are functions of four variables: the polar coordinates of the atom with

respect to the center of mass of the molecule, r , α , and β , and the internal dihedral angle γ :

$$V(r; \alpha, \beta, \gamma) = V_{\text{int}}(r; \gamma) + V_{\text{ext}}(r; \alpha, \beta). \quad (1)$$

The resulting model is that of an atom–semirigid-rotor interaction, suitable for elastic and inelastic collision simulations, both by quantum and classical mechanics.

2.2. THE INTERACTION: HYPERSPHERICAL HARMONICS REPRESENTATION

The potential energy surface of Eq. (1) for the interactions of H_2O_2 and H_2S_2 with rare gases can be given a mathematically faithful representation as a sum of hyperspherical harmonics [32, 33]. The range of the three angular variables spans a three-dimensional manifold isomorphic to S^3 (the sphere embedded in the four-dimensional Euclidean space \mathbf{R}^4), so the proper orthonormal expansion basis set can be given in terms of real hyperspherical harmonics $R_{M,M'}^\mu(\alpha, \beta, \gamma)$ (see, e.g., Refs. [40] and [41]). We defined [32] such a basis set in terms of real combinations of Wigner D -functions (which are in general complex), which are described and tabulated, for example, in Ref. [42]. The expansion is given by a sum of this basis functions multiplied by coefficients depending on the distance r :

$$V(r; \alpha, \beta, \gamma) = \sum_{\mu, M, M'} v_{M, M'}^\mu(r) R_{M, M'}^\mu(\alpha, \beta, \gamma), \quad (2)$$

where $\mu = 0, 1, 2, \dots$ and $M(M') = -\mu, -\mu + 1, \dots, 0, 1, \dots, \mu$, and the coefficients $v_{M, M'}^\mu(r)$ are the expansion moments depending on r only. The sum is truncated to a certain value of the index μ , which depends on the number of fixed atom–molecule configurations (e.g., a specific direction of a hypothetical incoming atom with respect to the oriented molecule) for which the potential energy is known (from previous ab initio calculations) as a function of r . For a recent general account of this type of expansions, see Ref. [43].

3. Simulations of Oriented Collisions

3.1. DEFINITIONS OF CROSS SECTIONS

To illustrate the manifestations in collisions of effects related to the chiral nature of the molecules, we have simulated collisions between rare gas atoms and hydrogen peroxide H_2O_2 or persulfide H_2S_2 . The

archetype of a chiral collision is one in which a chiral molecule is the target of a flux of atoms coming along specific directions with respect to the molecular target. This can be defined as an oriented collision, for which typical quantities, such as differential cross-sections can be defined and labeled on the basis of the orientations, besides the usual total energy and angular momentum and initial internal (e.g., roto-vibrational) states of the molecule. Let us adopt for the dynamics the same coordinates used in the representation of the rare gas–molecule interaction potential above [see Eq. (2)] to describe the collision. Again these are the distance r between the center of mass of the molecule and the atom, two spherical angles, α ($0 \leq \alpha < 2\pi$) and β ($0 \leq \beta \leq \pi$), defining the orientation of the molecule, and the dihedral angle γ , which is the internal torsion coordinate.

A directional cross-section can be defined as follows. The probability, determined from trajectories, for a given event i to occur upon an atom–molecule collision at collision energy E , impact parameter b , angles α and β defining the initial mutual orientation of the atom and molecule, and the angle γ fixing the molecule internal geometry is:

$$P_i(E, b, \alpha, \beta, \gamma, v, j) = \frac{N_i}{N}, \quad (3)$$

where the numbers v and j define the internal vibro-rotational state of the semirigid molecular rotor, N_i is the number of times that the event i has been detected in the collision trajectories, and N is the total number of trajectories. Integration over the impact parameters b gives the cross-section

$$\sigma(E, \alpha, \beta, \gamma, v, j) = 2\pi \int_{b=0}^{b=b_{\text{max}}} P_i(E, b, \alpha, \beta, \gamma, v, j) b db, \quad (4)$$

which depends on the internal molecular state and the orientation angles and where b_{max} is the maximum collision impact parameter, used as a truncation limit to skip, in the averaging process, trajectories leading to negligibly scattered products.

To emphasize the geometric properties of the collision events, which can be put into relationship with the chiral character of the two molecules, we find it convenient to define a function $\Theta(\Phi; E, b, \alpha, \beta, \gamma, v, j)$, which represents the scattering angle Θ that one would detect upon a collision oriented according to the angles α and β and characterized by energy and impact parameter E and b , the molecular state and geometry being given by the coordinate γ and

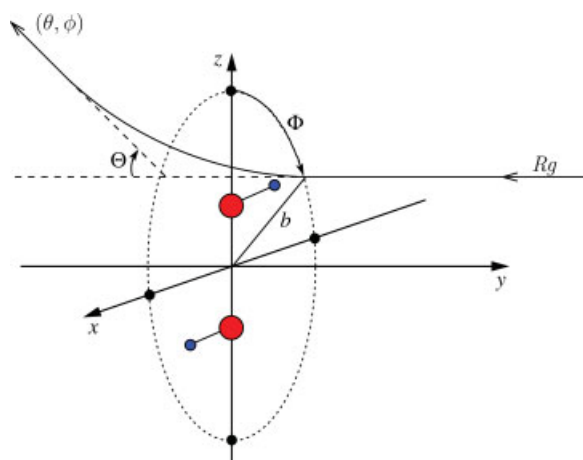


FIGURE 1. Sketch of the geometry of a typical oriented collision. The molecule (H_2O_2 or H_2S_2) is the target of a rare gas R_g coming from the y direction, perpendicular to the xz plane. The orientation of the molecular O–O and S–S bond defines the z axis. A circle in the xz plane corresponding to a given impact parameter b is shown along with a perpendicular line corresponding to the direction of the motion of the incoming atom, intersecting the circle in a point defined by the angle Φ (Section 3.1). The scattering angle Θ , between the initial and final directions of the motion, and the recoil direction, defined by the polar angles θ and ϕ , are indicated. [Color figure can be viewed in the online issue, which is available at www.interscience.wiley.com.]

the numbers v and j . The angle Φ is an Azimuthal angle spanning the annular ring between b and $b+db$ centered at the center of mass of the molecule, and perpendicular to the initial velocity vector of the atom. It is needed to identify the point of intersection of the line of the initial direction of the motion of the atom with the annular ring. In this way, Φ selects all the initial atom positions and velocities consistent with the given value of the impact parameter b and the orientation (α, β) of the collision. From a more physically meaningful point of view, the angle Φ makes the incoming atom flux draw a profile around the oriented molecular cross-section of radius b . It has to be noted that a sequence of collision trajectories with initial Φ varying smoothly and periodically between 0 and 2π mimics schematically a rotating flux of incoming atoms. The function Θ can in principle be calculated from trajectories as a function of the angle Φ for different enantiomers and for different handedness of the rotary motion of the incoming atom flux. Figure 1 sketches the collision geometry indicating the azimuthal angle Φ and the scattering angle Θ .

From $\Theta(\Phi; E, b, \alpha, \beta, \gamma, v, j)$, one can formally obtain a differential cross-section $I_{\alpha, \beta}^{v, j}(\Theta; E)$ for oriented collisions as follows:

$$I_{\alpha, \beta}^{v, j}(\Theta; E) = 2\pi \times \int_{b=0}^{b=b_{\max}} \int_0^{2\pi} \int_{\gamma_+}^{\gamma_-} \Theta(\Phi; E, b, \alpha, \beta, \gamma, v, j) b d\gamma d\Phi db, \quad (5)$$

where the integration is over b , Φ , and for γ , between the classical turning points of the internal torsion motion of the molecule, γ_+ and γ_- . Moreover, one can consider the probability of Eq. (3) for the scattering at a given value of the angle Θ , P_Θ , for a given energy and impact parameter E and b and a given orientation defined by the angles α and β , by the integration of the function $\Theta(\Phi; E, b, \alpha, \beta, \gamma, v, j)$ over Φ (see above):

$$P_\Theta(E, b, \alpha, \beta, \gamma, v, j) = \int_0^{2\pi} \Theta(\Phi; E, b, \alpha, \beta, \gamma, v, j) d\Phi \quad (6)$$

where, again, the numbers v and j define the internal vibro-rotational state of the molecule.

A natural extension of the above procedure is the generalization of the function Θ to a two-dimensional function defining the collision recoil direction. We will dedicate additional work to this aspect in the future. In this preliminary study (see Section 4), we consider the trajectory computed probability [Eq. (3)] for the scattering in a given solid angle defined by two polar angles θ and ϕ as a function of the angle Φ (see above) for a given collision energy and impact parameter E and b , and for a given initial roto-vibrational molecular state. The polar angles θ and ϕ , defining the recoil direction, are shown in Figure 1.

The above approach suggests that the trajectory study of oriented collisions, for the atom-molecule systems under focus here, can be reduced to obtaining Θ functions for a given impact parameter range, and to using them to calculate the oriented differential cross section by integration over the collision impact parameter and the internal torsional degrees of freedom of the molecule.

3.2. COMPUTATIONAL DETAILS

The initial conditions of the trajectories are generated by fixing the relative orientation of the molecule and the velocity vector of the atom, for a given impact

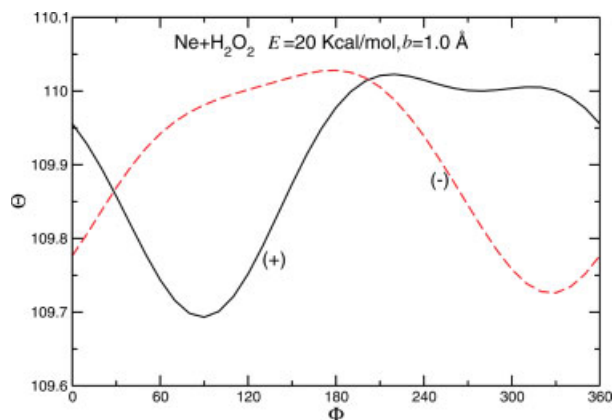


FIGURE 2. The scattering angle Θ (degrees) as a function of the angle Φ (see Fig. 1 and Section 3.1), for $\text{Ne} + \text{H}_2\text{O}_2$ at a collision energy of 20 kcal/mol and impact parameter $b = 1.0 \text{ \AA}$, for the two enantiomers of the molecule, indicated as (+) and (-). [Color figure can be viewed in the online issue, which is available at www.interscience.wiley.com.]

parameter and total energy. The molecule is taken to be at the configuration of minimum energy, according to the data in Table I. Then, the initial positions and velocities of the atom are changed varying the Φ angle (see Section 3.1) and consistently with the orientation of the collision. As pointed out in Section 3.1, the effects of a rotating flux of incoming atoms at a fixed energy and impact parameter can be reproduced by sequences of trajectories varying smoothly the initial value of the angle Φ , from 0 to 2π and from 0 to -2π , for left- and right-handed fluxes, respectively. Several values for the impact parameter b are generated randomly within a range from 0 to b_{max} (see Section 3.1) for a given collision energy. At the beginning of each trajectory, r (see Sections 2.1 and 2.2) is set to a large value so that initially the interaction between the atom and the molecule is negligible. This scheme permits, by extensive and massive calculations, to obtain converged oriented differential cross-sections according to Eq. (5).

4. Results

We have performed an ample set of calculations of collision trajectories for the $\text{Ne} + \text{H}_2\text{O}_2$ and $\text{Ne} + \text{H}_2\text{S}_2$ systems, at various collision energies E and orientations (see Sections 3.1 and 3.2).

Figure 2 represents the scattering angle Θ (see Section 3.1) as a function of Φ (to mimic the effect of a rotating flux of atoms) for the two enantiomers of the H_2O_2 molecule in the $\text{Ne} + \text{H}_2\text{O}_2$ system at

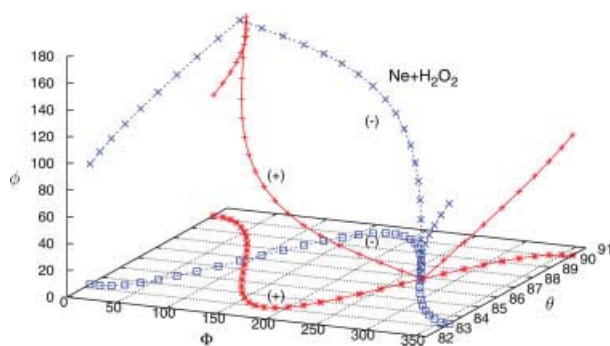


FIGURE 3. Plot of the recoil angles θ and ϕ (see Fig. 1 and Section 3.1) for $\text{Ne} + \text{H}_2\text{O}_2$ collisions as a function of the angle Φ for a collision energy of 120 kcal/mol and impact parameter $b = 1.0 \text{ \AA}$, for the (+) and (-) enantiomers of the molecule. Angles are in degrees. [Color figure can be viewed in the online issue, which is available at www.interscience.wiley.com.]

a collision energy of 20 kcal/mol (i.e., for a starting relative atom-molecule velocity U of $\sim 3600 \text{ m/s}$), for a collision impact parameter $b = 1.0 \text{ \AA}$ and for $\beta = 0$ (for $\beta = 0$ the value of α is undetermined). Figure 3 shows a three-dimensional plot of the collision recoil angles as a function of the angle Φ , for the two enantiomers of H_2O_2 in the $\text{Ne} + \text{H}_2\text{O}_2$ collisions at a collision energy of 120 kcal/mol ($U \approx 8900 \text{ m/s}$), for impact parameter $b = 1.0 \text{ \AA}$ and $\beta = 0$. As one can see from the 3D plot of the angles, the effect of changing the chirality of the target molecule can be also thought of as a change in the handedness of the

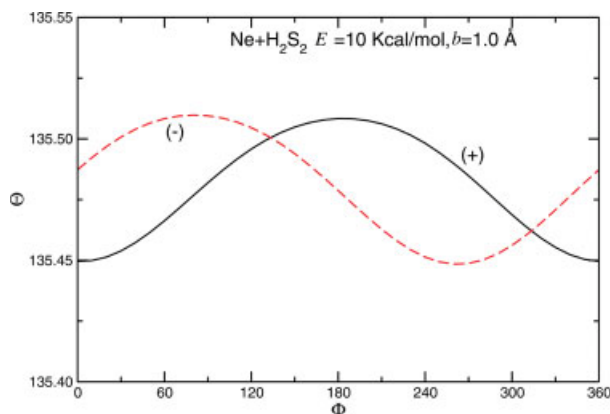


FIGURE 4. The scattering angle Θ (degrees) as a function of the angle Φ (see Fig. 1 and Section 3.1), for $\text{Ne} + \text{H}_2\text{S}_2$ collisions at an energy of 10 kcal/mol and an impact parameter $b = 1.0 \text{ \AA}$, for the two enantiomers of the molecule. [Color figure can be viewed in the online issue, which is available at www.interscience.wiley.com.]

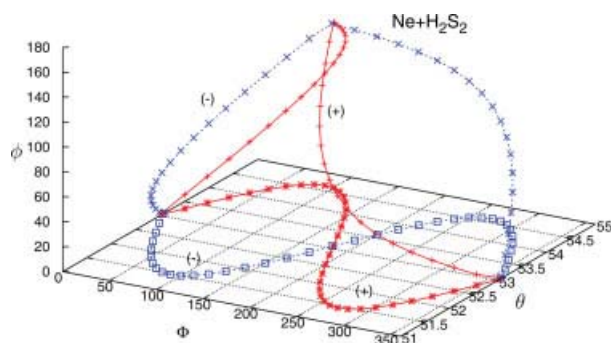


FIGURE 5. Plot of the recoil angles (see Fig. 1 and Section 3.1) for Ne + H₂S₂ collisions as a function of the angle Φ for a collision energy of 80 kcal/mol and an impact parameter $b = 1.0$ Å, for the two enantiomers of the molecule. Angles are in degrees. [Color figure can be viewed in the online issue, which is available at www.interscience.wiley.com.]

Cartesian reference system. This is a purely geometrical effect, whose consequences should be further investigated.

Figure 4 presents the scattering angle Θ as a function of the Φ angle for the two enantiomers of H₂S₂ in the Ne + H₂S₂ collisions, at a collision energy of 10 kcal/mol ($U \approx 2300$ m/s), for impact parameter $b = 1.0$ Å and $\beta = 0$. Figure 5, analogously to Figure 3, shows a three-dimensional plot of the collision recoil angles as a function of the angle Φ , for the two enantiomers of H₂S₂ in the Ne + H₂S₂ collisions at a collision energy of 80 kcal/mol ($U \approx 6600$ m/s), for impact parameter $b = 1.0$ Å and $\beta = 0$. Also here, from the 3D plot of the angles, one can see that the effect of changing the chirality of the target molecule is a change in the handedness of the Cartesian reference system.

The results shown are a clear indication of the fact that a rotating flux of atoms can actually distinguish (discriminate) between enantiomers of chiral molecules, which act like left- and right-handed screws.

5. Conclusions and Outlook

The hypothesis that chiral discrimination can follow from molecular collision mechanisms [3, 4] is largely unexplored. In this article, we presented a theoretical approach, based upon classical trajectory calculations, to simulate oriented collisions, namely collisions in which projectile rare gas atoms hit a simple chiral molecular target with a well defined

orientation with respect to the incoming atom direction. The formulation of the coordinates needed to specify initial conditions permits to simulate, at least qualitatively, the effects of a rotating flux of atoms of given handedness, colliding with the target chiral molecule. Far from being a direct attempt to shed light on how the mysterious homochirality phenomena can originate in nature, this work is a step towards the study of molecular collisions in a theoretical framework that takes into account explicitly of the molecular chirality. For effects in electron-molecule collisions, see [44–46]. Further steps will be in the direction of a general treatment of the chirality manifestation in collision dynamics, focusing the attention on those observables, which are potentially more directly related to chiral and stereochemical aspects, such as recoil scattering direction, angular momenta distribution, and the chirality inversion.

ACKNOWLEDGMENTS

It is a pleasure to have the opportunity that this article appears on the occasion of the celebration of the 60th birthday of Professor Sylvio Canuto, honoring his contribution to molecular dynamics.

References

1. Cline, D. B. European Review; Cambridge University Press: Cambridge, UK, vol. 13, 2005; p 49.
2. Rikken, G. L. J. A.; Raupach, E. Nature 2000, 405, 932.
3. Aquilanti, V.; Maciel G. S. Orig Life Evol Biosph 2006, 36, 435.
4. Aquilanti, V.; Grossi, G.; Lombardi, A.; Maciel, G. S.; Palazzetti, F. Phys Scri 2008, 78, 058119.
5. Ribó, J. M.; Crusats, J.; Sagués, F.; Claret, J.; Rubires, R. Science 2001, 292, 2063.
6. Matteson, D. S. Science 2003, 293, 1435.
7. Sun, B.; Lin, J.; Grosberg, A. I.; Grier, D. G. Phys Rev E 2009, 80, 010401.
8. (a) Speranza, M. Adv Phys Org Chem 2004, 39, 147–281; (b) Speranza, M.; Satta, M.; Piccirillo, S.; Rondino F.; Paladini, A.; Giardini, A.; Filippi, A.; Catone, D. Mass Spect Rev 2005, 24, 588; (c) Scuderi, D.; Paladini, A.; Satta, M.; Catone, D.; Filippi, A.; Piccirillo, S.; Laganà, A.; Speranza, M.; Giardini, A. Int J Mass Spect 2003, 223, 159; (d) Filippi, A.; Giardini, A.; Piccirillo, S.; Speranza, M. Int J Mass Spect 2000, 198, 137.
9. Aquilanti, V.; Bartolomei, M.; Pirani, F.; Cappelletti, D.; Vecchiocattivi, F.; Shimizu, Y.; Kasai, T. Phys Chem Chem Phys 2005, 7, 291.
10. Pirani, F.; Cappelletti, D.; Bartolomei, M.; Aquilanti, V.; Scotoni, M.; Vescovi, M.; Ascenzi, D.; Bassi, D. Phys Rev Lett 2001, 86, 5035.

11. Pirani, F.; Bartolomei, M.; Aquilanti, V.; Cappelletti, D.; Scotoni, M.; Vescovi, M.; Ascenzi, D.; Bassi, D.; Cappelletti D. *J Chem Phys* 2003, 119, 265.
12. Cappelletti, D.; Bartolomei, M.; Aquilanti, V.; Pirani, F.; Demarchi, G.; Bassi, D.; Iannotta, S.; Scotoni, M. *Chem Phys Lett* 2006, 420, 47.
13. Aquilanti, V.; Ascenzi, D.; Cappelletti, D.; Pirani, F. *Nature* 1994, 371, 399.
14. Aquilanti, V.; Ascenzi, D.; Cappelletti, D.; Pirani, F. *J Phys Chem* 1995, 99, 13620.
15. Aquilanti, V.; Ascenzi, D.; Cappelletti, D.; Fedeli, R.; Pirani, F. *J Phys Chem A* 1997, 101, 7648.
16. Pirani, F.; Cappelletti, D.; Bartolomei, M.; Aquilanti, V.; Demarchi, G.; Tosi, P.; Scotoni, M. *Chem Phys Lett* 2007, 437, 176.
17. Zhdanov, D. V.; Zadkov, V. N. *J Chem Phys* 2007, 127, 244312.
18. Quack, M.; Stohner, J. *Chirality* 2003, 15, 375.
19. Quack, M. *Angewandte Chemie Int Ed* 2002, 41, 4618.
20. Quack, M. *Angewandte Chemie Int Ed* 1989, 28, 571.
21. Faglioni, F.; D'Agostino, P. S.; Cadioli, B.; Lazzeretti, P. *Chem Phys Lett* 2005, 407, 522.
22. Bitencourt, A. C. P.; Ragni, M.; Maciel, G. S.; Aquilanti, V.; Prudente, F. *J Chem Phys* 2008, 129, 154316.
23. Aquilanti, V.; Ragni, M.; Bitencourt, A. C. P.; Maciel, G. S.; Prudente, F. *J Phys Chem A* 2009, 113, 3804.
24. Maciel, G. S.; Cappelletti, D.; Grossi, G.; Pirani, F.; Aquilanti, V. *Adv Quant Chem* 2008, 55, 311.
25. Maciel, G. S.; Bitencourt, A. C. P.; Ragni, M.; Aquilanti, V. *Chem Phys Lett* 2006, 412, 383.
26. Maciel, G. S.; Bitencourt, A. C. P.; Ragni, M.; Aquilanti, V. *Int J Quant Chem* 2007, 107, 2697.
27. Maciel, G. S.; Bitencourt, A. C. P.; Ragni, M.; Aquilanti, V. *J Phys Chem A* 2007, 111, 12604.
28. Daza, M. C.; Dobado, J. A.; Molina, J. M.; Salvador, P.; Duran, M.; Villaveces, J. L. *J Chem Phys* 1999, 110, 11806.
29. Daza, M. C.; Dobado, J. A.; Molina, J. M.; Villaveces, J. L. *Phys Chem Chem Phys* 2000, 2, 4094.
30. Molina, J. M.; Dobado, J. A.; Daza, M. C.; Villaveces, J. L. *J Mol Struct Theochem* 2002, 580, 117.
31. Elango, M.; Parthasarathi, R.; Subramanian, V.; Ramachandran, C. N.; Sathyamurthy, N. *J Phys Chem A* 2006, 110, 6294.
32. Barreto P. R. P.; Vilela A. F. A.; Lombardi A.; Maciel G. S.; Palazzetti F.; Aquilanti V. *J Phys Chem A* 2006, 111, 12754.
33. Maciel G. S.; Barreto P. R. P.; Palazzetti F.; Lombardi A.; Aquilanti V. *J Chem Phys* 2008, 129, 164302.
34. Aquilanti, V.; Cornicchi, E.; Teixidor, M. M.; Saendig, N.; Pirani, F.; Cappelletti, D. *Angewandte Chemie Int Ed* 2005, 44, 2356.
35. Cappelletti, D.; Vilela, A. F. A.; Barreto, P. R. P.; Gargano, R.; Pirani, F.; Aquilanti, V. *J Chem Phys* 2006, 125, 133111.
36. Redington, R. L.; Olson, W. B.; Cross, P. C. *J Chem Phys* 1962, 36, 1311.
37. Marsden, C. J.; Smith, B. J. *J Chem Phys* 1988, 92, 347.
38. Hunt, R. H.; Leacock, R. A.; Peters, C. W.; Hecht, K. T. *J Chem Phys* 1965, 42, 1931.
39. Herbst, E.; Winnewisser, G. *Chem Phys Lett* 1989, 155, 572.
40. Aquilanti, V.; Cavalli, S.; Grossi, G. *J Chem Phys* 1986, 85, 1362.
41. Aquilanti, V.; Cavalli, S.; Coletti, C.; Di Domenico, D.; Grossi, G. *Int Rev Phys Chem* 2001, 20, 673.
42. Varshalovich, D. A.; Moskalev, A. N.; Khersonskii, V. K. *Quantum Theory of Angular Momentum*; World Scientific: Singapore, 1988.
43. Palazzetti, F.; Elango, M.; Lombardi, A.; Grossi, G.; Aquilanti, V. *Int J Quant Chem* (in press).
44. Busalla, A.; Blum, K.; Thompson, D. G. *Phys Rev Lett* 1999, 83, 1562.
45. Musigmann, M.; Busalla, A.; Blum, K.; Thompson, D. G. *J Phys B: At Mol Opt Phys* 2001, 34, 79.
46. Musigmann, M.; Busalla, A.; Blum, K.; Thompson, D. G. *J Phys B: At Mol Opt Phys* 2001, 34, 2679.